Photon Generation in an Electromagnetic Cavity with a Time-Dependent Boundary

C. M. Wilson,[1] T. Duty,[2] M. Sandberg,[1] F. Persson,[1] V. Shumeiko,[1] and P. Delsing[1]

[1]*Microtechnology and Nanoscience, Chalmers University of Technology, S-41296, Göteborg, Sweden*
[2]*School of Mathematics and Physics, University of Queensland, St. Lucia, QLD 4072, Australia*

(Received 13 June 2010; revised manuscript received 3 November 2010; published 2 December 2010)

We report the observation of photon generation in a microwave cavity with a time-dependent boundary condition. Our system is a microfabricated quarter-wave coplanar waveguide cavity. The electrical length of the cavity is varied by using the tunable inductance of a superconducting quantum interference device. It is measured at a temperature significantly less than the resonance frequency. When the length is modulated at approximately twice the static resonance frequency, spontaneous parametric oscillations of the cavity field are observed. Time-resolved measurements of the dynamical state of the cavity show multiple stable states. The behavior is well described by theory. Our results may be considered a preliminary step towards demonstrating the dynamical Casimir effect.

DOI: 10.1103/PhysRevLett.105.233907 PACS numbers: 42.65.Lm, 05.45.−a, 42.79.Gn, 85.25.Cp

Photons, in contrast to electrons, interact only very weakly with each other [1]. However, effective interactions can be induced when photons interact with a nonlinear media. In many cases, these effective interactions result in so-called parametric processes which are important in widespread technological applications and also in fundamental studies of quantum electrodynamics [2,3]. In the optical regime, the nonlinearities are generally bulk properties of materials or plasmas. In the rf and microwave regime, they are often created by lumped-element electrical devices [4].

Alternatively, it has been proposed that parametric processes can be observed in a system that is essentially linear but where a boundary condition of the electromagnetic field can be changed rapidly in time. For instance, this is the central theoretical problem in the field of the dynamical Casimir effect (DCE) [5,6]. One striking prediction of the DCE is that real photons can be generated out of the vacuum by the changing boundary condition. The experimental system often imagined in describing the DCE is a cavity with a moving mirror. Estimates suggest that this is technically a very challenging route to pursue, however [7,8]. Therefore, a number of authors have suggested alternative approaches including modulating the electrical properties of the cavity [9–13] or other nonadiabatic perturbations [14,15].

Regardless of the source of the interactions, the quantum behavior of parametric systems has been of great interest. For example, the quantum dynamics of parametric oscillators (POs) has been described theoretically in several different contexts [16,17]. In fact, the DCE can be mapped to the quantum version of the PO in special cases [18]. A driven PO can exist in a number of stable dynamical states. In a PO with negligible loss, it is predicted that quantum tunneling between the states is possible, leading to the formation of so-called Schrödinger cat states. In POs with more loss, it is predicted that quantum tunneling will always be hidden by a distinct process known as quantum activation [19]. Quantum activation is an incoherent process, driven by relaxation (spontaneous emission), that nonetheless leads to ''over-the-barrier'' switching of the dynamical state, even at zero temperature. None of these quantum predictions have been conclusively observed in experiment.

To this end, superconducting systems are interesting for several reasons: Josephson junctions can be used to make the resonator's frequency tunable over a wide range; nonlinearities can be easily designed at a desired strength; and they have very little dissipation. Parametric Josephson devices were pioneered in the 1980s by Yurke *et al.* [20] and have recently regained interest [21–26]. It has recently been suggested that these are promising systems for studies of the DCE [12,13].

In this work, we have studied tunable, high-Q superconducting cavities. They are $\lambda/4$ coplanar waveguide cavities fabricated on-chip (Fig. 1). The cavities are made tunable by incorporating a superconducting quantum interference device (SQUID), used as a parametric inductance. The cavities are cooled such that $k_B T \ll \hbar\omega_0$, ω_0 being the resonance frequency, implying that the average number of thermal photons is well below 1. When we strongly drive the magnetic flux through the SQUID at $\sim 2\omega_0$, we observe the generation of microwave photons in the cavity [Fig. 2(a)]. As explained below, we do not claim to have observed the DCE, although our results may be considered a preliminary step towards this.

Our cavities are spatially extended systems described by a wave equation. The modulated SQUID imposes a time-dependent, nonlinear boundary condition on the wave equation. For a static but nonlinear boundary condition, an exact, analytical solution is already not possible, although approximate solutions can be found in the form of coupled oscillators [27]. Treating time-dependent boundary conditions is one of the essential aspects of the

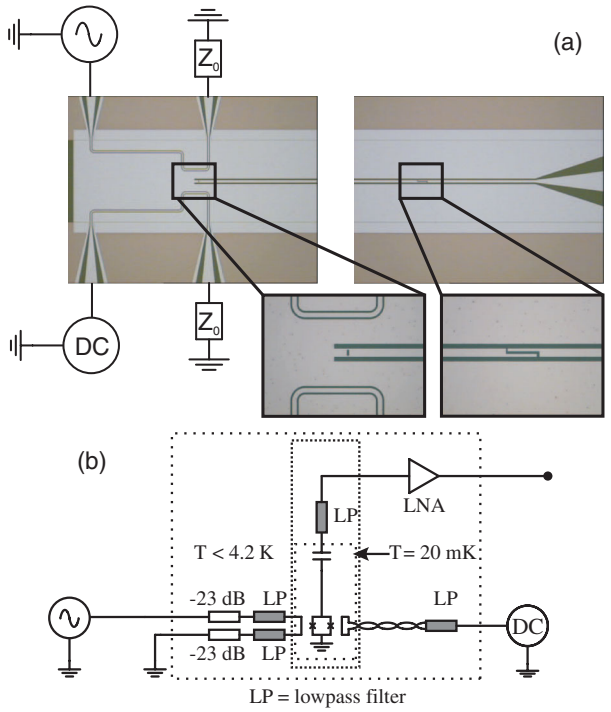

FIG. 1 (color online). (a) A micrograph of a $\lambda/4$ cavity. Metal layers appear light and the substrate dark. The cavity's length is $d = 5.56$ mm. The center conductor is 13 μm wide with a gap of 7 μm to the ground planes. The cavity is probed through a small coupling capacitance (right enlargement) while the other end is terminated to ground through a SQUID (left enlargement). Changing the external magnetic field through the SQUID loop changes the boundary condition of the cavity. (b) Simplified block diagram. The cavity is measured by using a circulator and a cold amplifier. The magnetic field is applied via on-chip control lines, one for high frequency and one for dc.

dynamical Casimir problem. For a general time-dependent boundary condition, the system can be reduced to an effective set of coupled modes where both the mode frequencies and the couplings are time-dependent [28,29]. If the cavity is designed such that the static mode frequencies are not multiples of each other, then we can find an approximate solution when the modulation frequency is twice the static resonance frequency of one of the modes. In this case, the dynamics of the isolated, pumped mode can be reduced to those of a PO [18]. Starting from a pure vacuum state in the cavity, the appearance of parametric oscillations in this mode is then one example of the DCE.

Some care must therefore be taken in describing the dynamics of the system, taking into account the difficulties and subtleties mentioned above. In addition, ω_0 must be designed to be much less than the plasma frequency of the bare SQUID, so that its internal dynamics can be ignored [13]. In particular, this guarantees that we do not excite parametric oscillations in the SQUID itself. All that said, we do find experimentally that the dynamics of the system can be described by the equation for a parametric oscillator with the appropriate set of effective parameters, i.e., Eq. (1). The dynamical variable is the canonical flux of the cavity $\Phi = \Phi_0\varphi/2\pi = \int_{-\infty}^{t} V dt'$, where V is the voltage and Φ_0 is the flux quantum.

A PO can be described by the differential equation [17]:

$$\partial_{tt}\varphi + 2\Gamma\partial_t\varphi + [\omega_0^2 + F\cos(\omega_p t)]\varphi + \gamma\varphi^3 = \xi(t), \tag{1}$$

where F is the amplitude of the frequency modulation, $2\Gamma = \omega_0/Q$ is the linewidth of the resonance and describes the damping of the system, and γ represents the dominant nonlinearity of the system, the so-called Duffing term. $\xi(t)$ represents a mean-zero noise term that leads to activated switching.

We derive an expression for F by linearizing the tuning curve of the cavity $\omega_0^2 = \omega_b^2[1 + r(x)]^{-2}$ with respect to the external flux $x = \Phi_B/\Phi_0$ [24]. Here, $r(x) = L_s(x)/dL_l$, where L_s is the SQUID inductance, d is the physical length of the cavity, and L_l is its inductance per unit length. We find $F = 2\pi\tan(\pi x_{\rm dc})(\omega_0^3/\omega_b)rx_{\rm ac}$, where the subscripts dc and ac distinguish between the static bias point and ac pump amplitude. In our system, γ arises from the coupling of the current in the excited cavity to the SQUID. Following Ref. [27], we find $\gamma = -\omega_0^2\delta^3/\pi$ with $\delta = -(\pi/2)r/(1 + r)$.

Once the system has been put in the form of (1), its behavior can be understood in terms of the slow quadrature variables q_1 and q_2, where $\varphi(t) = q_1(t)\cos(\omega_p t/2) - q_2(t)\sin(\omega_p t/2)$. In the rotating frame, the dynamics of q_1 and q_2 are determined by the metapotential

$$g(q_1, q_2) = \frac{\Omega}{2}(q_1^2 + q_2^2) + \frac{\zeta}{2}(q_2^2 - q_1^2) + \frac{\beta}{4}(q_1^2 + q_2^2)^2, \tag{2}$$

where $\Omega = \frac{1}{\Gamma}(\frac{\omega_p}{2} - \omega_0)$ is the normalized detuning, $\zeta = F/2\Gamma\omega_p$ is the normalized drive strength, and $\beta = 3\gamma/4\Gamma\omega_p$ is the normalized nonlinearity. Below the pump threshold value of $\zeta = 1$, this potential has only one minimum centered at the origin. Thus the system does not oscillate. For small detunings, as the threshold is crossed, two symmetric minima develop, yielding two stable, oscillating states phase shifted by 180°. As the pump is blue detuned, we reach a bifurcation point where the two stable states merge into a single "quiet" state at the origin. If the pump is instead red detuned, another bifurcation point is reached where a metastable state develops at the origin. The system then has three states: the two π-shifted oscillating states and a quiet state.

The cavity and SQUID are fabricated in aluminum by using double-angle evaporation. We previously showed that the cavity frequency can be changed much faster than the lifetime of the photons in the cavity [24]. The samples were mounted in a magnetically shielded sample holder in a dilution refrigerator with a base temperature of ~20 mK.

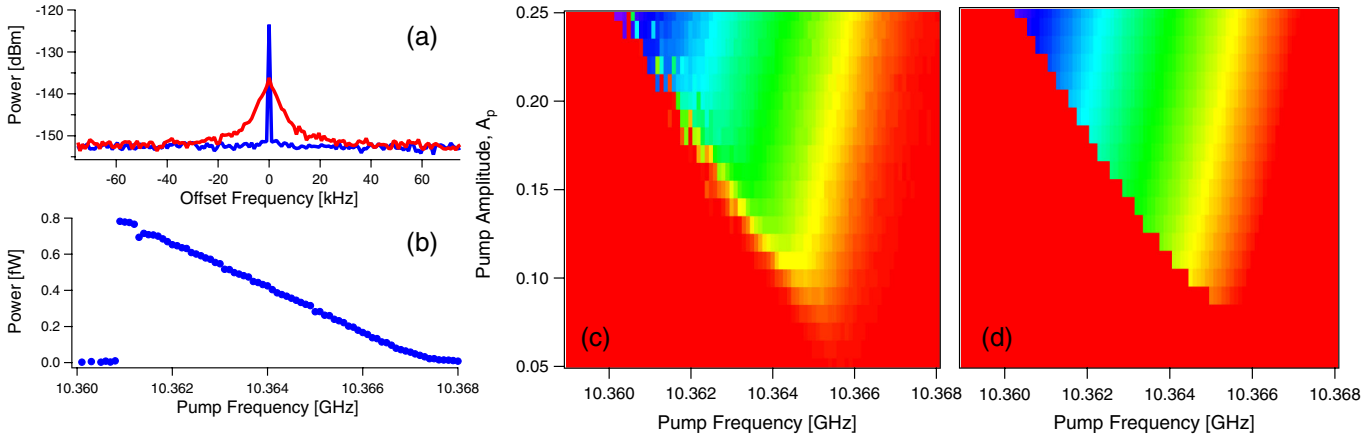

FIG. 2 (color online). The output of the pumped cavity. (a) Two output power spectra referred to the cavity output, for different working points–wider (red) peak: $f_p = 10.3651$ GHz, $A_p = 0.11$; narrower (blue) peak: $f_p = 10.3637$ GHz, $A_p = 0.23$. The offset frequency is centered at $f_p/2$. The widths of the peaks are the switching rates between different states (see Fig. 3). (b) Integrated output power as a function of f_p for $A_p = 0.23$. The amplifier noise power has been subtracted. The predicted linear dependence on detuning from the bifurcation point is clear. (c) Integrated output power as a function of A_p and f_p. The increased noise near the left boundary is due to the slow switching of the output power in this region. (d) Theoretical fit from solving Eq. (1). The color scales are the same in both plots.

The measurements of the cavities were done by using a cryogenic amplifier at 4.2 K that had a nominal noise temperature of 4 K. The samples were connected to the amplifier via a circulator mounted on the mixing chamber. The resonance frequencies and the Q values of the samples were characterized by coupling a weak probe signal to the cavity via the circulator. For the photon generation experiments, no signal was applied to the cavity, but a flux pumping signal at approximately twice the resonance frequency was applied to the fast flux line. The output of the cavity was recorded by using a vector digitizer.

We have studied the pumped cavities as a function of both pump amplitude and frequency. In Fig. 2, we show the output power of a pumped cavity with $\omega_0/2\pi = 5.1828$ GHz and $Q = 8900$. The pump amplitude A_p is scaled such that $20\log(A_p)$ is the power at the microwave generator in dBm. In Fig. 2(d), we show the steady state solution to (1), namely, $\langle\varphi^2\rangle = (\sqrt{\zeta^2 - 1} - \Omega)/2\beta$. In the range where this solution is imaginary or negative, we take the solution $\langle\varphi^2\rangle = 0$. To scale the y axis of the theory, we define $F = F_A A_p$ and calculate a value of $F_A = 9.9 \times 10^{18}$ s^{-2} by using a dc calibration of the pump flux coupling. To scale the z axis (color scale), we calculate $\gamma = 1.9 \times 10^{17}$ s^{-2} and estimate the total gain of our amplifier chain, which is nominally $G = 75$ dB. To fit the data, we allow F_A and G to vary. We find a best fit for $F_A = 3.0 \times 10^{18}$ s^{-2} and $G = 73$ dB. We note that, since the power is proportional to G/γ, these parameters are not independently constrained. It is not surprising that we would find a different value for F_A, since the cable loss and flux mode structure should be different for the dc calibration and the $\sim$10 GHz pump flux. Keeping that in mind, we conclude that the agreement is good.

The data are clearly asymmetric with respect to frequency. This is explained in the following way. At the blue detuned bifurcation point $\Omega_B^+ = +(\zeta^2 - 1)^{1/2}$, the oscillating states vanish and only the quiet state is stable. In contrast, at the red detuned $\Omega_B^- = -(\zeta^2 - 1)^{1/2}$, the quiet state emerges but is only metastable, with an occupation probability that is exponentially small. The oscillations stop only when the occupation probability of the quiet state becomes significant. In Ref. [17], it is estimated that this happens for $\Omega \approx -4\zeta$. We find that $\Omega = -3.4\zeta$ agrees better with the data.

We visualize the dynamics of the system by making histograms of the measured quadrature pairs (q_1, q_2). The maxima of the histograms then correspond to the stable points of the metapotential. In this way, we map out the metapotential (2). In Fig. 3, we plot histograms of (q_1, q_2) sampled at 1 MHz. In agreement with theory, we find that the system has three qualitatively different conditions: (i) one stable state where the magnitude is zero, (ii) two stable states symmetric about zero, and (iii) three states which combine (i) and (ii). We can also clearly see the softening of the metapotential just before the system bifurcates. We observe switching between the different states which may be caused by thermal activation, quantum activation, or quantum tunneling [19,30]. A detailed analysis of the rates will be the topic of a future paper.

We thus find a good agreement between the response of a cavity with a time-dependent boundary condition and the theory of a PO. This experimentally confirms one of the fundamental predictions of the DCE literature [18]. Furthermore, the quantitative agreement is good evidence that the source of photon generation is in fact the time-dependent boundary.

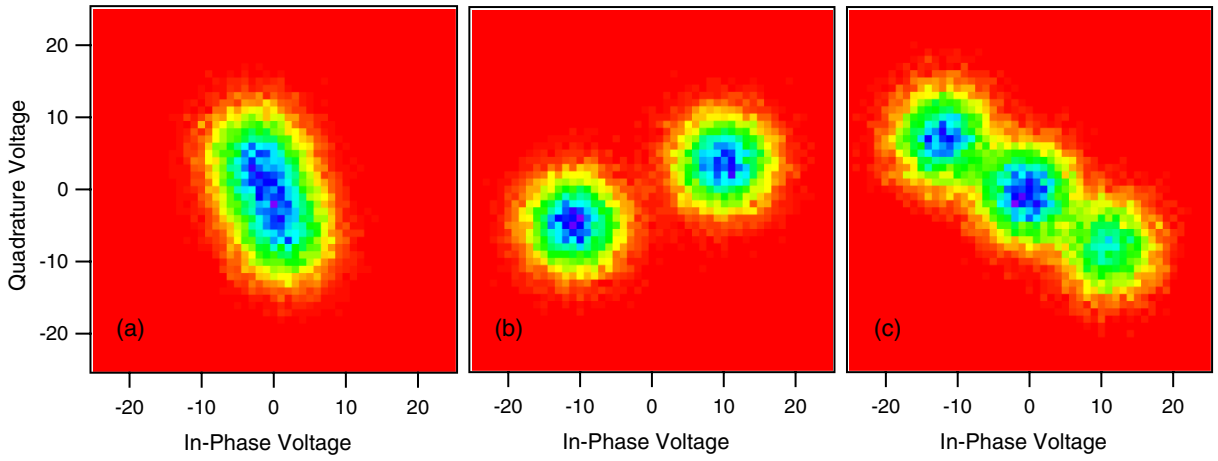

FIG. 3 (color online). Exploring the metapotential. 2D histograms of measured in-phase q_1 and quadrature q_2 voltages for three different working points. (a) Just below threshold near zero detuning, the metapotential softens in one direction and we observe a noise ellipse. (b) Above threshold and red detuned, the system has bifurcated, exhibiting two finite-amplitude oscillating states. These states have equal amplitude but are shifted by 180° in phase. (c) When the pump is far red detuned, a quiet state can coexist with the oscillating states, in agreement with theory. The noise circles in (b) and (c) are dominated by the measurement amplifier. The phase rotations between the three images are also instrumental artifacts.

It is fair to ask whether we can interpret these results in terms of the DCE. This is essentially a question of whether quantum fluctuations or thermal fluctuations initiated the cavity oscillations. We cannot conclusively distinguish between the classical and the quantum results, since we measure only the steady state oscillations which are insensitive to the initial conditions. In the future, it may be possible to distinguish the quantum and classical results by observing the system's transient response. Alternatively, the steady state solutions are different if the cavity is removed and the SQUID is left to modulate the boundary condition of an open transmission line [13].

We thank M. Dykman and G. Johansson for useful discussions. The devices were made at the nanofabrication lab at Chalmers. Support came from the Swedish VR, the Wallenberg foundation, the ERC, and the EU projects EuroSQIP and SCOPE.

[1] E. Iacopini and E. Zavattini, Phys. Lett. **85B**, 151 (1979).
[2] D. Bouwmeester *et al.*, Nature (London) **390**, 575 (1997).
[3] L. Wu *et al.*, Phys. Rev. Lett. **57**, 2520 (1986).
[4] B. Yurke *et al.*, Phys. Rev. A **39**, 2519 (1989).
[5] G. Moore, J. Math. Phys. (N.Y.) **11**, 2679 (1970).
[6] S. Fulling and P. Davies, Proc. R. Soc. A **348**, 393 (1976).
[7] C. Braggio *et al.*, Europhys. Lett. **70**, 754 (2005).
[8] W. Kim, J. Brownell, and R. Onofrio, Phys. Rev. Lett. **96**, 200402 (2006).
[9] E. Yablonovitch, Phys. Rev. Lett. **62**, 1742 (1989).
[10] Yu. Lozovik, V. Tsvetus, and E. Vinogradov, JETP Lett. **61**, 723 (1995).
[11] V. Dodonov, A. Klimov, and D. Nikonov, Phys. Rev. A **47**, 4422 (1993).
[12] J. R. Johansson *et al.*, Phys. Rev. A **82**, 052509 (2010).
[13] J. Johansson *et al.*, Phys. Rev. Lett. **103**, 147003 (2009).
[14] G. Günter *et al.*, Nature (London) **458**, 178 (2009).
[15] S. DeLiberato, C. Ciuti, and I. Carusotto, Phys. Rev. Lett. **98**, 103602 (2007).
[16] G. Milburn and C. Holmes, Phys. Rev. A **44**, 4704 (1991).
[17] M. I. Dykman *et al.*, Phys. Rev. E **57**, 5202 (1998).
[18] V. Dodonov, Phys. Lett. A **207**, 126 (1995).
[19] M. Marthaler and M. I. Dykman, Phys. Rev. A **73**, 042108 (2006).
[20] B. Yurke *et al.*, Phys. Rev. Lett. **60**, 764 (1988).
[21] E. A. Tholen *et al.*, Appl. Phys. Lett. **90**, 253509 (2007).
[22] M. A. Castellanos-Beltran *et al.*, Nature Phys. **4**, 929 (2008).
[23] B. Abdo *et al.*, Europhys. Lett. **85**, 68 001 (2009).
[24] M. Sandberg *et al.*, Appl. Phys. Lett. **92**, 203501 (2008).
[25] A. Palacios-Laloy *et al.*, J. Low Temp. Phys. **151**, 1034 (2008).
[26] T. Yamamoto *et al.*, Appl. Phys. Lett. **93**, 042510 (2008).
[27] M. Wallquist, V. S. Shumeiko, and G. Wendin, Phys. Rev. B **74**, 224506 (2006).
[28] A. Dodonov and V. Dodonov, Phys. Lett. A **289**, 291 (2001).
[29] R. Schutzhold, G. Plunien, and G. Soff, Phys. Rev. A **57**, 2311 (1998).
[30] I. Serban and F. K. Wilhelm, Phys. Rev. Lett. **99**, 137001 (2007).